Science of the Total Environment 705 (2020) 135774

Contents lists available at ScienceDirect

Science of the Total Environment

journal homepage: www.elsevier.com/locate/scitotenv

Sensitivity of soil moisture to precipitation and temperature over China: Present state and future projection

Bowen Zhu [a,b], Xianhong Xie [a,b,*], Shanshan Meng [a,b], Chuiyu Lu [c], Yi Yao [a,b]

[a] State Key Laboratory of Remote Sensing Science, Jointly Sponsored by Beijing Normal University and Institute of Remote Sensing and Digital Earth of Chinese Academy of Sciences, Beijing 100875, China
[b] Beijing Engineering Research Center for Global Land Remote Sensing Products, Institute of Remote Sensing Science and Engineering, Faculty of Geographical Science, Beijing Normal University, Beijing 100875, China
[c] China Institute of Water Resources and Hydropower Research, State Key Laboratory of Simulation and Regulation of Water Cycle in River Basin, Beijing 100038, China

HIGHLIGHTS

- SM is more sensitive to climate changes in the humid area than it in other regions.
- A sensitivity-based approach is proposed to perform SM projection.
- South West and North China are likely to experience a SM decline in the future.

GRAPHICAL ABSTRACT

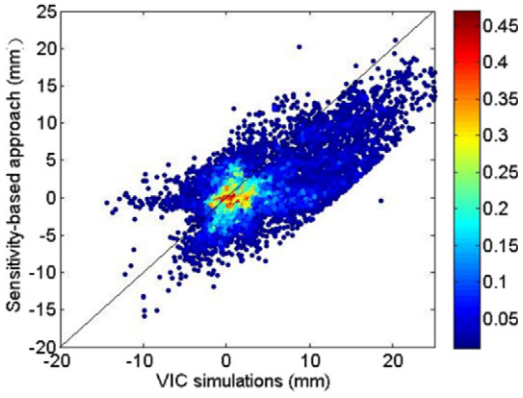

ARTICLE INFO

Article history:
Received 5 September 2019
Received in revised form 21 November 2019
Accepted 24 November 2019
Available online 30 November 2019

Editor: Jay Gan

Keywords:
Soil moisture
Sensitivity
Climate change
Land surface modeling

ABSTRACT

Soil moisture (SM) is a key variable in the climate system as it regulates the latent and sensible heat partition and influences eco-hydrological processes. A few studies have highlighted the increasing frequency of SM droughts at the river basin scale in China, however, little is known about the SM response to precipitation (P) and near-surface temperature (T) at national and regional scales. In this study, the long-term SM dynamics based on a sophisticated land surface hydrological model (i.e., the Variable Infiltration Capacity, VIC) were identified after model evaluation. A simple but effective sensitivity-based approach was developed to quantify the elasticity (ε) and sensitivity (S) of SM to P and T, and the SM was projected for the near future at the regional scale. The results indicate that China has experienced slightly wetter soil conditions during the past five decades and the SM has increased in the arid and semi-arid regions of China, i.e., the North East (0.11 mm/yr) and the North West (0.047 mm/yr). The elasticity and the sensitivity of SM are the highest in the humid region (i.e., South East China), indicating that small increases of P and T are likely to induce considerable changes in the SM relative to other regions. The sensitivity-based approach could perform SM estimation similar to the complex VIC modeling. This approach projected that North China ($-5.05 \pm 2.31\%$) and South West China ($-5.95 \pm 2.04\%$) are likely to experience drying with a considerable decline in SM due to reduction in P and rise in T in the near future period from 2020 to 2050. The slightly wet soil conditions in the past and a drying future scenario may imply a contrasting consequence for the regional-scale hydrological cycles.

* Corresponding author at: Beijing Normal University, China.
E-mail address: xianhong@bnu.edu.cn (X. Xie).

https://doi.org/10.1016/j.scitotenv.2019.135774
0048-9697/

1. Introduction

Soil moisture (SM) in the climate system imposes considerable impacts on water, energy, and biogeochemical cycles (Seneviratne et al., 2010). It can regulate vegetation dynamics (Alamusa et al., 2017) and also plays an irreplaceable role in maintaining the sustainability of ecosystems in arid regions (Zhang et al., 2017). The SM controls interaction of the land with the atmosphere and its dynamics are dominated by a range of geophysical parameters such as regional climate (Li et al., 2016b), soil properties and vegetation density (She et al., 2014). Thus, it is important to quantify SM variability and its response to climatic factors considering the changing environmental conditions.

China has experienced significant climate change with regard to temperature (T) and precipitation (P) in the recent decades. For example, the North East region of China is warming with T increase of 0.38 °C per decade (Chen et al., 2011), southern China has experienced a T increase at the rate of 0.29 °C/decade and a slight decrease in P by 6.07 mm/decade (Liu et al., 2016). The changes in P and T can reshape the water balance (Touhami et al., 2015) and have a considerable impact on streamflow, groundwater, and SM dynamics (Stoll et al., 2013).

The dynamics of SM are primarily driven by P and evapotranspiration (Jia et al., 2018; Rushton et al., 2006), and both of which have a coupled interaction with rising T. As a result, SM has been severely altered to adapt to the warming climate system. In the recent years, SM has shown significant downward trends in northern and northeastern China (Wang et al., 2011). However, in the context of global change, most research has mainly focused on hydrological budgets changes and the response of vegetation and agriculture to climate change during the past decades, while the sensitivity of SM to climate change and SM changes in the future in China have not yet been adequately understood.

In general, SM can be estimated by three approaches: in-situ measurements, remote sensing (RS), and hydrological modeling (Jia et al., 2018). In-situ measurements can provide the most reliable estimates at point scale but are limited by the number stations worldwide including regions in China (Cao et al., 2015). In contrast, the RS technique is capable of monitoring SM states at large scales, however, the RS data products only represent the first few centimeters of the soil layer (Zribi, 2003), therefore the products may hold considerable biases (Jia et al., 2018). Moreover, most RS products are available for a short time period. For example, the products from the Soil Moisture and Ocean Salinity (SMOS) are available since November 2009 and the Soil Moisture Active Passive (SMAP) data can be obtained for the period after January 2015 (Karthikeyan et al., 2017a; Karthikeyan et al., 2017b; Mishra et al., 2017). Alternately, hydrological modeling is capable and widely used to assess the SM dynamics (Koch et al., 2016). In particular, field and basin-scale hydrological models have been frequently employed to study eco-hydrological processes (Li et al., 2016b; She et al., 2014). Li et al. (2016b) applied Soil and Water Assessment Tool (SWAT) model to explore spatio-temporal variations in SM of the Yellow River basin of China. She et al. (2014) used the Soil Water-Carrying Capacity for Vegetation (SWCCV) model as a diagnostic tool to explore the distinguishing effects of vegetation density and land use on soil water dynamics in the Loess Plateau, northwestern China. Large-scale hydrologically-based land surface models are more suitable to diagnose SM related processes at regional or national scales (Jia et al., 2018).

Based on land surface models and related climate forcing data, SM and other hydrological variables can be projected for future scenarios. Extensive studies have employed off-line modeling to assess the impacts of climate change on SM, in which land surface models were driven by outputs from global climate models (Tang and Dennis, 2014). (Amin et al., 2017; Chiristensen and Lettenmaier, 2007). Nevertheless, this approach entails considerable computational costs and rigorous data management since reliable projections depend on repeated model runs when new climate datasets are released (Vano et al., 2012; Vano and Lettenmaier, 2013). Moreover, only SM trends and changes instead of the sensitivity of SM to P and T were examined at the regional scale from previous studies. To alleviate this issue, Vano and Lettenmaier (2013) proposed a sensitivity-based method to explore the response of runoff to climate change. This method produces first-order estimates to determine the bounds of uncertainties with regard to long-term runoff response to climate change. It is able to effectively capture the relationships between hydrological budgets and climate factors, and it is also flexible to allow SM projections after reasonable adaptions (Vano et al., 2012; Vano and Lettenmaier, 2013).

The main objectives of this study were: (1) to identify the spatio-temporal variability in the SM across China during the 1960–2014 and its correlations with P and T; (2) to quantify the precipitation elasticity (ε) and the temperature sensitivity (S) of SM; and (3) to project the SM through a simple sensitivity-based method under future climatic conditions. A large-scale distributed hydrological model, i.e., the variable infiltration capacity (VIC) model (Liang et al., 1994; Liang et al., 1996) was used to investigate the response of the SM to climate change in China. Based on this land surface modeling, the sensitivity-based approach was extended to conduct SM projections.

This paper is structured as follows. The inputs and validation data for the VIC model and methods are introduced in Section 2. The climate change, SM response and projection are presented in Section 3, followed by a discussion of evidence from other studies and limitations in Section 4. Finally, Section 5 summarizes the conclusions.

2. Data and methods

2.1. Large-scale hydrological model

The VIC model is a macro-scale model which resolves the hydrology and energy balance within each grid cell at each time step (Liang et al., 1994; Liang et al., 1996; Liang and Xie, 2003). It has been successfully applied to many hydrological simulations during droughts and floods and for water resource management. Additionally, it has also been applied at scales ranging from a watershed (Liang and Xie, 2001) to regional and global scales (Nijssen et al., 2001; Tang and Dennis, 2014; Tang and Piechota, 2009; Xie et al., 2015).

The meteorological forcing data for the VIC model will be described in Section 2.2. The data for the VIC parameters regarding vegetation types were derived from the University of Maryland global cover classifications (Hansen et al., 2010) and soil texture was based on the dataset obtained from the Food and Agriculture Organization of the United Nations (FAO, 1998) which have been successfully used in Zhang et al. (2014). The model was run at a spatial resolution of 0.25° × 0.25° for the period of 55 years (1960–2014). It was cold started on January 1, 1960 and spun up for the period off 5 years from 1960 to 1964. The model state at the end of this period served as the initial condition for all subsequent model experiments. The soil profile was divided into three layers. The depth of the top layer was constant (0.1 m) and thicknesses of the other two layers were designated by the soil properties.

2.2. Meteorological forcing data

In this study, the meteorological forcing data for the VIC model included daily P, wind speed, and maximum, minimum, and mean Ts. These forcing data were produced from 752 stations of observations which were obtained from the China Meteorological Administration (CMA) for 1960–2014. The meteorological station observations were quality controlled and interpolated at a resolution of 0.25° × 0.25° into a gridded data set (Xie et al., 2015). The same CMA data and the interpolation method to generate gridded forcing data have been successfully applied to hydrological simulations of the VIC model in previous studies (Xie et al., 2015; Xie et al., 2007). Thus, the input forcing data created in this study were expected to be of high quality and suitable for conducting SM simulations for China.

2.3. Data for model evaluation

In this study, the SM data used for model evaluation included two datasets: In-situ observations and RS retrievals. The in-situ data were obtained from the CMA from 1991 to 2014. The dataset consisted of SM values at different depths (i.e. 10 cm, 20 cm, 50 cm, 70 cm and 100 cm) at a sampling interval of 10 days during the crop growing season. Only the data for the 10 cm and the 100 cm depths, which can capture surface and deep-depth changes of the SM, were considered to validate the VIC results. After data quality control, 156 stations (Fig. 1) with data length > 10 years were selected for model evaluation. Their spatial distribution covers most areas in China, and each is close to a target grid cell.

The RS SM data were available from the European Space Agency (ESA)'s Water Cycle Multimission Observation Strategy and Climate Change Initiative projects (ESA-CCI SM). The ESA-CCI SM consisted of three data sets: the "active product" was based on backscatter measurements, the "passive product" was derived from brightness and T measurements, and the "combined product" was a blended product based on the former two datasets. In this study, the combined product was adopted, as it has the consistent spatial resolution (0.25°) and a daily time step spanning period ranging from 1978 to 2013. This product has been extensively evaluated worldwide, including regions in China, with ground-based observations (Wang et al., 2016). To ensure comparability with the sensing depth of the satellite sensors, simulated SM within the upper 10 cm was considered (Dorigo et al., 2015).

2.4. Sensitivity analysis and projection methods

Dynamics of SM are sensitive to P and T. According to the method proposed by Vano et al. (2012), we developed a simple sensitivity-based approach to reflect the SM responses to changes in P and T, respectively. As described in Eq. (1), the precipitation elasticity ε is a measure of the fractional change in SM divided by the fractional change in P. Similarly, the temperature sensitivity S is a measure of percent change in SM divided by the per degree change in T (Eq. (2)).

$$\varepsilon = \frac{SM_{hist+\Delta P} - SM_{hist}}{\Delta P} \cdot \frac{1}{SM_{hist}} \tag{1}$$

$$S = \frac{SM_{hist+\Delta T} - SM_{hist}}{\Delta T} \cdot \frac{1}{SM_{hist}} \tag{2}$$

where SM_{hist} is the SM from a baseline simulation with the historical climate condition, which represents the long-term average results (i.e. 1960–2014). $SM_{hist+\Delta P}$ and $SM_{hist+\Delta T}$ are from simulation scenarios with perturbations of precipitation and temperature, respectively (Vano and Lettenmaier, 2013; Vano et al., 2015). To detect the stability of ε and S, multiple simulation scenarios were designed with different perturbations of P ($\Delta P = -20\%, -10\%, 1\%$, and 10%) and increments of T ($\Delta T = 0.1$ °C, 1 °C, 2 °C, and 3°C) relative to the historical P and T conditions.

As the SM is primarily driven by P and T, it was assumed to be a function of P and T, i.e., f(P, T). Based on the work by (Vano et al., 2012), a simple sensitivity-based approach (Eq. (3)) was used to estimate SM responses to future climate changes in China.

$$\begin{aligned} SM_{future} &= \mathrm{f}(P_{future}, T_{future}) \\ &= \mathrm{f}(P_{hist}, T_{hist}) + \frac{\partial \mathrm{f}}{\partial \mathrm{P}}\Delta P + \frac{\partial \mathrm{f}}{\partial \mathrm{T}}\Delta T + R_n \\ &= SM_{hist} + (\varepsilon \cdot SM_{hist})\Delta P + (S \cdot SM_{hist})\Delta T + R_n, \end{aligned} \tag{3}$$

where SM_{future}, $P_{future}$and T_{future} are future SM, P and T projections, respectively, ΔP and ΔT denote changes in P and T, relative to their historical values (P_{hist}, T_{hist}), and R_n is the Taylor's expansion remainder which can be neglected. This approach can also be defined as the response of a particular hydrological model to a known quantum of climate change (Jones et al., 2006). In this study, we first evaluated the performance of this sensitivity-based approach in comparison to the VIC modeling and subsequently, we applied the approach to project future SM changes.

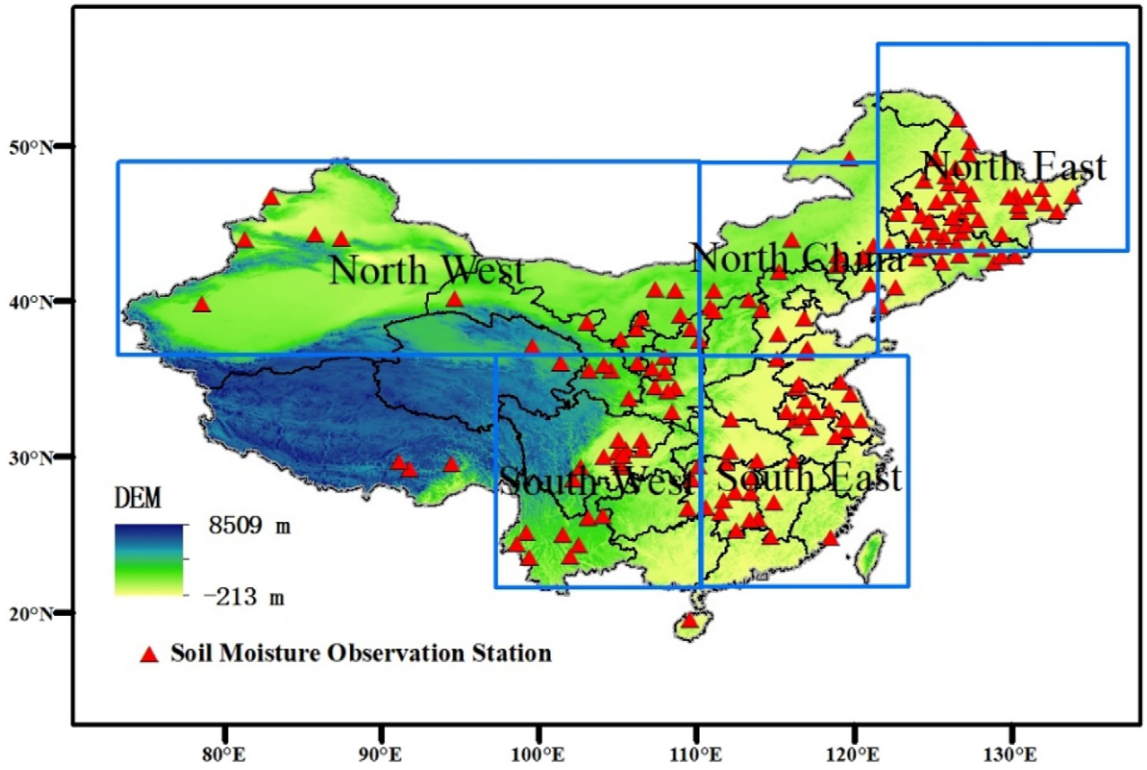

Fig. 1. The distribution of elevation in China and the SM observation stations. The area was divided into five regions: North East (NE), North China (NC), North West (NW), South East (SE), and South West (SW).

3. Results

3.1. Evaluation of SM simulations

3.1.1. Evaluation using in-situ observations

The VIC performance has been extensively evaluated with respect to streamflow and evapotranspiration in China. Xie et al. (2007) used streamflow data from 33 stations across China to calibrate and validate the VIC model and acceptable performance was achieved for streamflow simulations. Zhang et al. (2014) conducted VIC simulations across China and evaluated the VIC model with regard to streamflow. Xie et al. (2015) indicated the VIC model to show favorable evapotranspiration (as well as streamflow) estimation (for stations in the Three-North region of China) when evaluated using eddy covariance. However, to our best knowledge, the VIC model for SM estimation in China has not been adequately evaluated.

This study focused on evaluating the VIC for SM estimation instead of streamflow and evapotranspiration. First, the SM simulation was conducted using in-situ observations. Considering the scale difference between the VIC simulations (0.25° grid scale) and the in-situ observations (point scale), the simulated SM was interpolated to the observation sites using the bilinear interpolation approach. Moreover, at each observation site, the VIC simulated SM was linearly interpolated to the depths of 10 cm and 100 cm which represent depths at which measurements were conducted. To represent the agreement between the simulation and the in-situ observations, two commonly used metrics were computed, i.e., the Spearman rank correlation coefficient (R) and the percentage bias. The coefficient R is an indication of temporal agreement and the bias was used to measure the relative difference between the simulation and the observations at sites.

Fig. 2 shows the two metrics for the 156 observation sites. With regard to the correlation coefficient, R values for most stations were >0.5 and the highest reached around 0.9. The bias ranged from −10%–10% for both soil depths of 10 cm and 100 cm. Additionally, the bias for the 10 cm depth was smaller than that for the 100 cm depth, indicating that the VIC model better simulated the upper-layer soil. Despite discrepancies between simulations and observations at some sites, the VIC generally provided acceptable estimates of SM in the top and deep layers.

3.1.2. Evaluation using RS data

The ESA-CCI SM data were used to evaluate the VIC simulated top-layer (10 cm) SM, focusing on the temporal and spatial agreement between the two SM estimates. The absolute differences (simulation values minus the ESA-CCI SM values) and their relative differences ($\frac{absolute\ difference}{ESA-CCI\ SM}$) were calculated for each grid cell.

The average seasonal difference and standard deviations between the VIC simulations and the ESA-CCI SM data for China were quite small (Fig. S1). The differences between the two datasets were higher in summer (June to August) when most P was input to subsequently supplement the SM, while a better agreement was indicated in spring (March, April, and May) and winter (December, January, and February). With regard to the spatial differences (Fig. 3), SM estimates derived from the RS data were higher than those simulated by the VIC for most of South East China across all seasons and the relative bias ranged from −10% to −20%. As shown in Fig. 3, the SM in south China was underestimated by VIC in the summer and autumn, partly because the VIC model only simulated SM in the natural condition, while the impact of human activities, such as irrigation, was not considered. The spatial

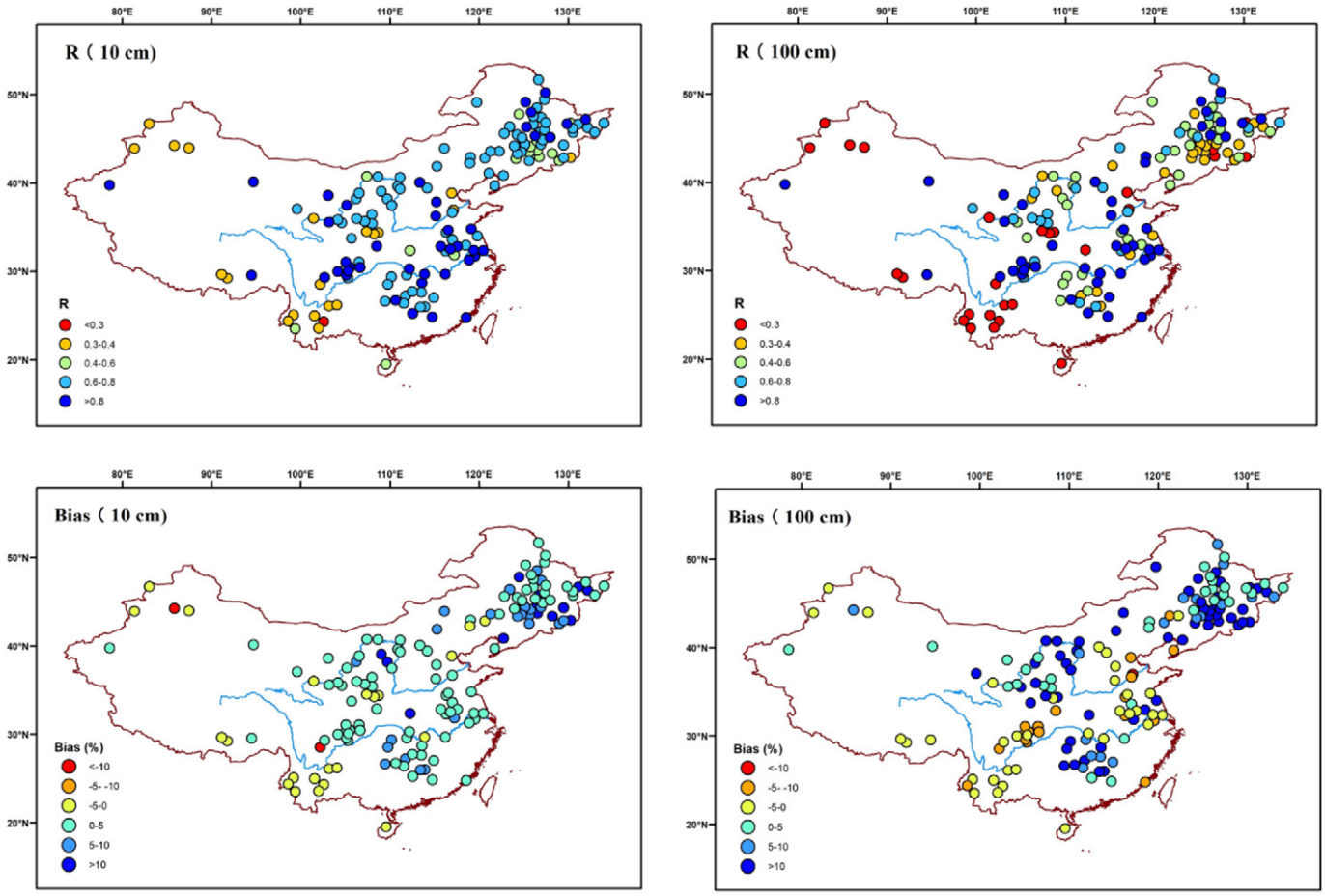

Fig. 2. Correlation coefficient and bias between observations and simulations. A total of 156 stations were selected to make comparisons.

pattern did not show an obvious seasonal change (a larger bias in South than North China in each season) implying that the VIC simulated SM gave the same seasonal pattern as the ESA-CCI SM data. Please note the area (difference > 20%) is less 5% of the whole area, so the model performance is acceptable for such a large domain. Additionally, it was evident that the ESA-CCI SM data covered most areas in autumn (September, October, and November), while data were missing during the other months. Overall, the results indicate that the VIC model produced reliable SM estimates to a certain degree.

3.2. Changes in P, T and SM

To explore the spatial distributions of P, T, and SM trends based on historical forcing data and simulations, the area of China was divided into five regions: North East, North West, South East, South West, and North China (Fig. 1). Each region represented a relatively-unique climate zone and enabled a better understanding of the SM changes under different circumstance (Wang et al., 2011). The Tibetan Plateau was excluded in this study because considerable SM simulation uncertainties were possibly caused by the forcing data and the snow and ice melting formulation in the VIC model. The Mann-Kendall test was used to detect the annual trends for P, T, and SM from 1960 to 2014.

As shown in Fig. 4 and Table 1, P decreased over North China (−1.12 mm/yr) and South West China (−2.10 mm/yr) but increased dramatically in North West China (0.94 mm/yr), a pattern consistent with the estimates from Zhai et al. (2005). With regard to T, considering the current global warming, most regions in China exhibited a considerable increase in T (0.025 °C/yr) and North China experienced stronger warming than South China (Yan et al., 2013).

The trends of simulated SM for the total soil depth were generally consistent with the P trends, except for some areas in the South East coast where SM indicated a downward trend while P showed an upward change. This may be caused by a significant increase in the T. South West China indicated the highest downward trend in SM (−0.20 mm/yr) and the highest increase in SM (0.047 mm/yr) was observed in North West China. Liu et al. (2015) analyzed the SM during the growing season in North China and concluded that the SM had decreased by 6% since 1983. These spatial distributions were similar to those indicated by the ESA-CCI SM data as indicated by the Mann-Kendall test and Spearman's Rho test (Qiu et al., 2016). Therefore, SM trends were affected by P as well as T (Wang et al., 2011).

3.3. Correlation at regional scale

The SM correlations with P and T at a regional scale were identified based on the *R* (Fig. S2). All six correlation coefficients for SM and P were >0.6. The highest *R* appeared in the North West with a value of 0.90. This region is characterized by low annual P (165 mm) compared to the other regions, therefore, the recharge of the SM relied heavily on the P. The SM correlations with T for all regions were smaller than those observed with P. Moreover, the SM and T exhibited a negative relationship since soil water evaporation would be accelerated due to the rising T. These results indicate that changes in P had positive influences and T imposed negative effects on the SM dynamics despite the different correlations in the five regions which were partly attributed to the discrepancy of the climatic background. Therefore, the sensitivity of SM to P and T may vary in different regions. The SM sensitivity is further discussed in Section 3.4.

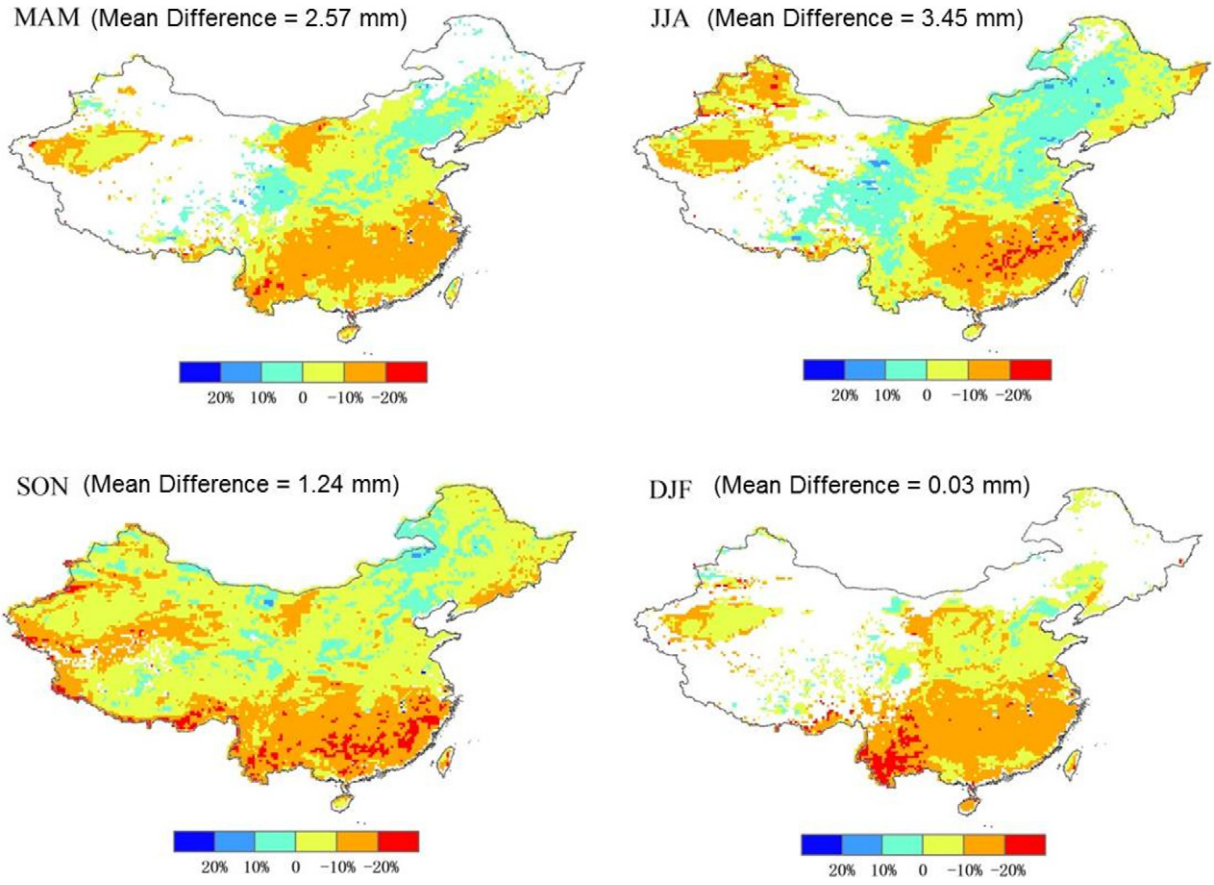

Fig. 3. The spatial differences in SM between the VIC simulations and the ESA-CCI SM estimates (simulation values minus the ESA-CCI SM values) for the four seasons. The blank areas are areas without available ESA-CCI SM data.

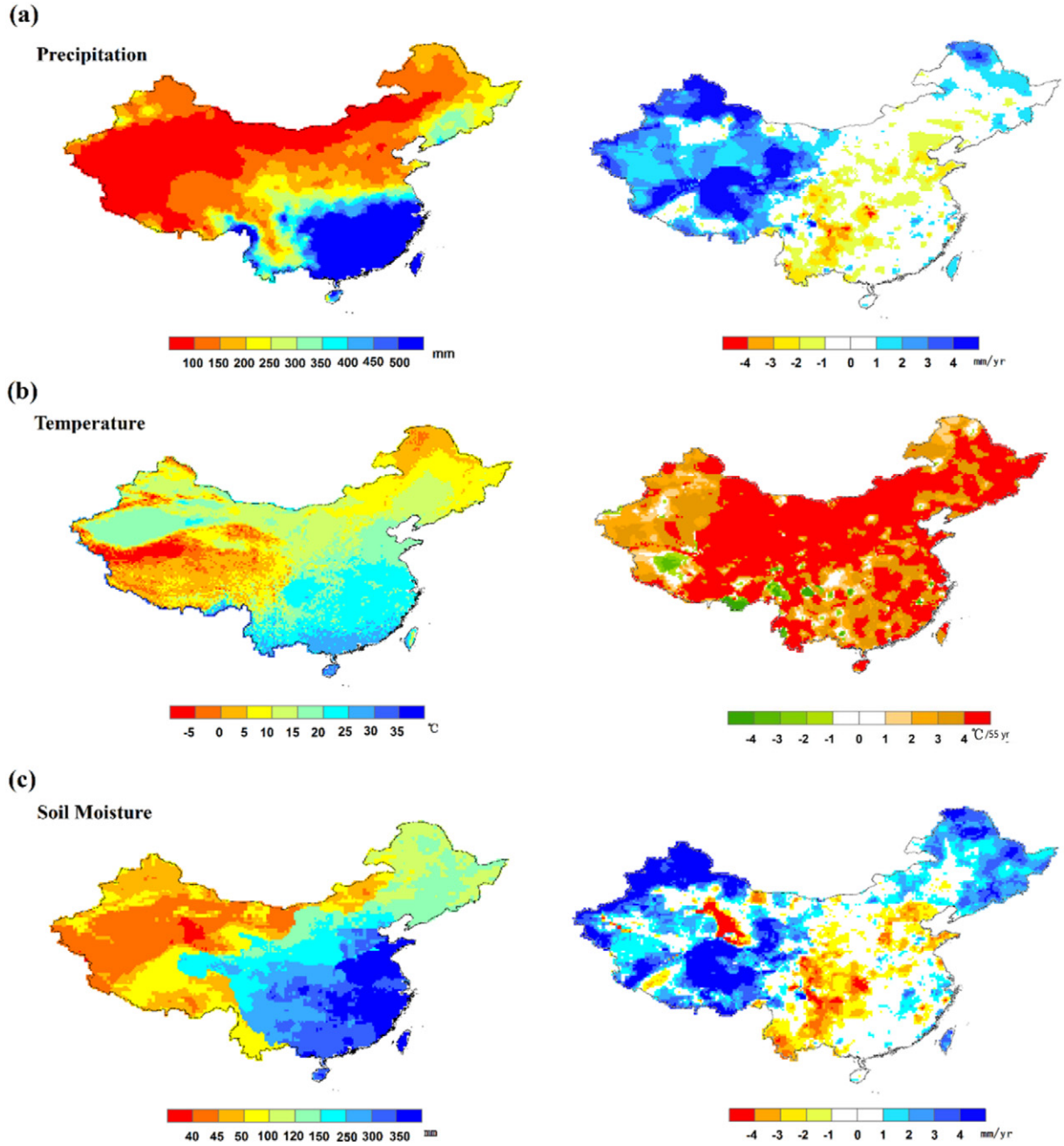

Fig. 4. Annual averages (left) and trends (right) in P, T and SM.

3.4. Sensitivity and projection

3.4.1. SM sensitivity

We examined the SM sensitivity to climate change at regional scale considering substantial uncertainties in SM estimation at each VIC simulation grid cell. Moreover, we also applied the sensitivity approach to make a regional-scale SM projection. The precipitation elasticity ε was calculated using Eq. (1) by perturbing P at 80%, 90%, 101%, and 110% relative to the historical mean values. The temperature sensitivity *S* was estimated using Eq. (2), using 0.1, 1, 2, and 3 °C increases to test the effect of different change increments.

Fig. 5 indicates that the average ε varied from 0.15 in North West (arid climate zone) to 0.48 in South East (humid climate zone), indicating that a 1% increase in P could increase the SM by 0.15% to 0.48%. Therefore, the SM in the North West indicated a lower ε in comparison to the South West. *S* presented negative values and showed an upward trend with increasing increments of T. North West China showed the lowest absolute *S* value, indicating that the SM was more stable when T changed compared to other regions. In contrast, South East China indicated the highest absolute *S*, suggesting the largest SM sensitivity to T. Therefore, the SM in the humid region of China was more sensitive to

Table 1
Annual trends in P, T and SM in each region estimated by Mann-Kendall test.

Area	Precipitation (mm/yr)	Temperature (°C/yr)	SM (mm/yr)
North East	0.061	0.025	0.11
North West	0.94	0.031	0.047
South East	−0.59	0.018	0.069
South West	−2.10	0.015	−0.20
North China	−1.12	0.029	−0.13
China	0.22	0.025	0.0065

P and T while the SM in the arid region of China showed less sensitivity to P and T. In humid region, please also note that the soil profile can store more water because of well planted vegetation and high density agriculture (Thompson et al., 2010). Therefore, the soil profile gains and loses water more easily, indicating high sensitivity of SM to P and T.

The variation of ε (0.1 to 0.5) was smaller than that of *S* (from −1 to −5), therefore, the average value of *ε* with regard to different levels of P changes reasonably captured the regional-scale ε. However, *S* presented a large variation with regard to different levels of T increases, therefore, its average was not sufficient to represent the sensitivity. In this study, a linear regressive function was employed to approximate the *S* (Table S1) The five functions presented a favorable approximation of variations in *S* and the coefficient of determination $R^2 > 0.7$. North China presented the largest slope according to the aggressive function, which implies that the magnitudes of SM changes were more evident when different T increments were used in this region. This is illustrated by the climate change challenges, such as water shortage, food demand, and high carbon emissions, experienced by North China (Zhang et al., 2015)

3.4.2. Evaluation of the sensitivity-based approach

The above-mentioned sensitivity analysis indicates that it is possible to use the simple sensitivity-based approach to make SM projections instead of using the more complex land surface hydrological modeling (e.g., the VIC modeling). Therefore, the sensitivity-based approach using VIC simulations was evaluated for the historical period. Specifically, the values of *ε* and *S* were calculated from 1960 to 1984 to construct the sensitivity-based model (Eq. (3)). Subsequently, this model was used to make projections for the period between 1990 and 2014. The projection accuracy could be evaluated using the VIC simulated SM values from 1990 to 2014.

The average ε and the *S* regressive function for each region were presented in Table S2. ε and *S* indicated values different to the ones shown in Table S1 because they were calculated for different time periods, as indicated previously. However, the differences were very small. For example, South East China was most sensitive to P and T changes. Therefore, the SM sensitivity was found to be robust to a certain degree. Based on the estimates of ε and the *S*, the SM projection could be made from 1990 to 2014.

Fig. 6 (a) and (b) show the spatial distribution of SM changes from the sensitivity-based approach as well as the VIC simulations which, in most areas, ranged between −5 mm and 5 mm. The average changes in the SM in China in comparison to the past decades were 3.02 mm and 2.04 mm as estimated by the sensitivity-based approach and VIC model, respectively. Although, there were some differences in North West China where the results derived by the sensitivity method were higher than those obtained from the VIC simulations, the SM changing pattern was largely consistent between the two methods. As indicated in Fig. 6 (c), the sensitivity-based approach generally presented a good relationship with the VIC model projections with R value and Nash Suffice coefficient of 0.67 and 0.38, respectively, indicating the capability of the sensitivity method to project the SM reasonably well. Fig. 6 (d) shows the specific changes in the SM of the five regions and their spatial distributions across China. The results deduced from the sensitivity method as well as the VIC simulations for North East and North West China indicate that the SM has increased relative to the past 25 years, while the other regions indicated a decline in the SM. On the other hand, South West and North China indicated negative values from 1960 to 2014 and the decreasing results indicate an accelerating declining phenomenon in the overall trend of the SM in both areas. Therefore, the sensitivity-based approach is capable of reasonable SM projection.

3.4.3. Projection for future patterns

The reasonable projection capability of the sensitivity-based approach, as described previously, enables it to project the SM patterns for the near-future from 2020 to 2050. Therefore, the sensitivity-based model was re-constructed with new ε and *S* values that were computed from simulation data from 1960 to 2014 (Fig. 5 and Table S1). Based on this model, along with the projected future changes in T and P, the regional-scale SM pattern was projected for the period from 2020 to 2050. The future changes in T and P were abstracted from Leng et al. (2015) and Zhang et al. (2015). Given the substantial uncertainties in the projected T and P at grid cell scale, we focused on regional-scale SM projection.

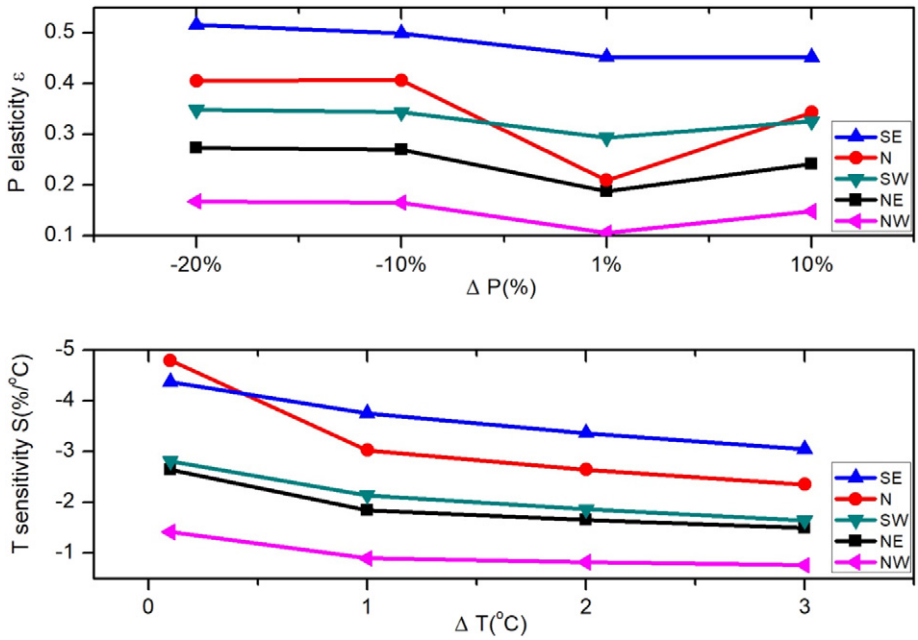

Fig. 5. Annual precipitation elasticity and temperature sensitivity in the different regions.

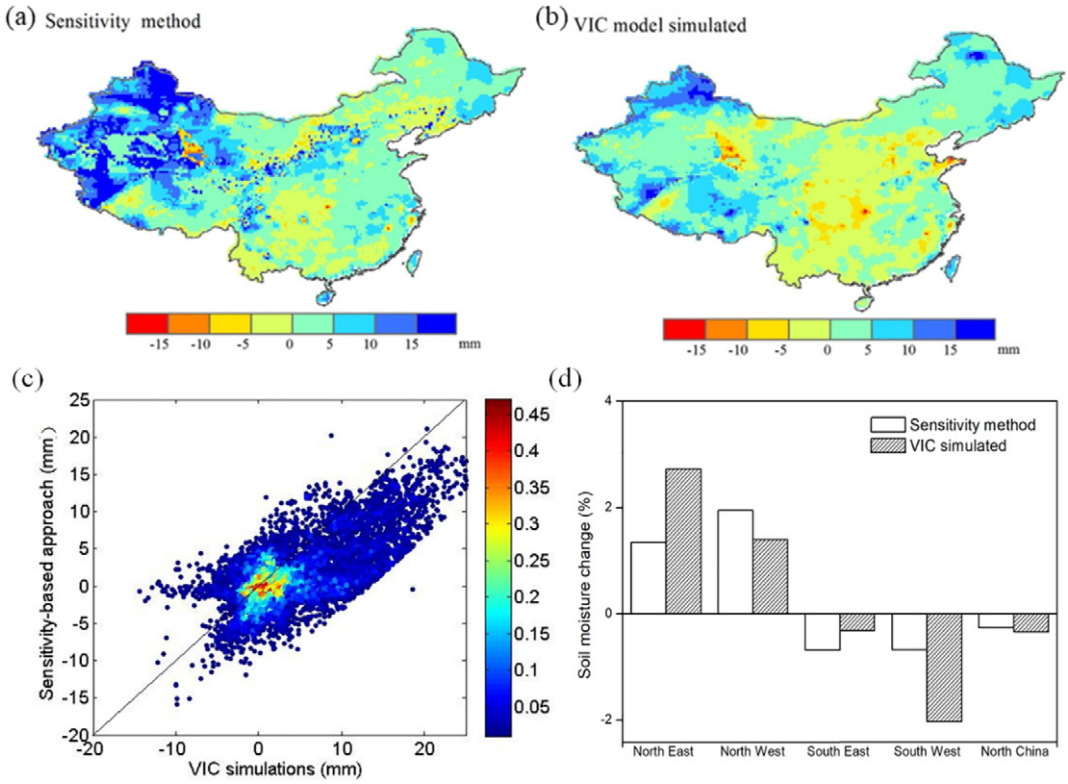

Fig. 6. SM changes from 1990 to 2014 and 1960–1984 obtained from (a) the sensitivity method, and (b) the VIC model. (c) Comparisons of predicted changes of annual average SM from the VIC simulation and the sensitivity-based approach. The bar shows the density of all grids. (d) SM changes in different regions.

According to the model projections, western and northern China are likely to experience an increase in future P by 5% to 15% (Leng et al., 2015). Additionally, the model results showed a decrease in P of up to 10% in major areas of Central and parts of South West China, and the largest decrease is expected in southwestern and northeastern China (Leng et al., 2015). The multi-model ensembles predict a warmer climate for the entire country with increase in the T for the period from 2020 to 2050 ranging from 1 to 4 °C.

Based on these projections, different probable magnitudes changes in P and T (Table 2) were evaluated to subsequently foresee the future SM changes (ΔSM_{future}) relative to the historical SM in each region. Table 2 shows the results of annual SM changes under future climate scenarios. The results indicate that the range of reduction of SM in contrast to the historical values will vary across most arid and semi-arid regions, and the South West will experience the largest SM decrease as the evaporation will likely increase and the relative humidity of air will continually decrease in this region resulting in intensified droughts (Wang et al., 2014). Unlike the runoff pattern of the dry North, wetter conditions in the South will be exacerbated in the future (Wang et al., 2012); the SM will probably only increase in the humid region (South East) and the arid region (North West) while other places, such as the semi-arid region, will experience a decrease in the SM which will induce more agricultural drought events (Leng et al., 2015).

Table 2
Annual SM changes for the period 2020–2050.

Area	ΔP	ΔT	ΔSM_{future}
North East	5%–10%	2–3 °C	−1.97% (±0.91%)
North West	5%–15%	2–3 °C	−0.36% (±0.87%)
South East	10%–15%	1–2 °C	0.65% (±2.68%)
South West	−10%–−5%	1–3 °C	−5.95% (±2.04%)
North China	−5%–0	1–2 °C	−5.05% (±2.31%)

4. Discussions

4.1. SM response to P and T

This study identified the climate and the SM changes in China from 1960 to 2014 based on the VIC simulations. Recently, several studies have assessed hydrological responses in the context of global climate change by using in-situ measurements, RS data, and modeling techniques.

As evidenced by ground weather stations in the arid region of North West China, P indicated a significant increasing trend at a rate of 0.61 mm/year from 1960 to 2010 (Li et al., 2016a). In the southeastern river basin, a warming-wetting tendency was observed from 1957 to 2013, while the central regions tended to be warmer and drier (Tian et al., 2016). Over the same period, the mean warming rate in the Yellow, Yangtze, and Pearl River basins, which cover the majority China, was 0.22 °C/decade (Tian and Yang, 2017). Overall, these trends are highly consistent with our results. In addition, only a few studies have reported the SM changes over a longer time period at regional and national scales.

Unlike previous studies, this study conducted model evaluations for the SM using in-situ observations and RS data and identified the SM response to climate change over the past 55 years. The results indicate that the SM has experienced a period of decline during the past years in North Central and North East China.

Climate change is one of the major challenges with regard to water security in China (Piao et al., 2010). To have a better understanding of changes of water budgets in the near future is benefit for water resource management. Several studies have focused on changes in runoff (Wang et al., 2012), food security (Blum, 2013) and water demands (Jiang, 2015) in the future. However, the response of SM to climate change has not been sufficiently discussed (Qiu et al., 2016), although SM is a crucial factor in water and energy exchange and it controls the partition

of P between runoff and infiltration. The hydrological sensitivity-based approach is capable of projecting future SM changes under different climate change scenarios. Nakaegawa (2017) used a multi-model ensemble analysis that showed significant increases in the SM in a North West inland area, and significant decreases were projected in southern and northern China which are consistent with our future projections. Our findings are also consistent with the research of Tao et al. (2003) that indicated water-related challenges in the coming decades in the northern China plain and North East China due to the expected SM deficit.

4.2. Potential limitations

In this study, the VIC model was utilized to estimate the SM changes. Like several other studies (Haddeland et al., 2007; Wu et al., 2014), the VIC model simulations only considered natural forcing, i.e., climate change, rather than anthropogenic actives and land cover changes such as afforestation practices, urbanization, and agricultural water management. The changes in land use and land cover may be significant as the population growth and climate change, which will bring influences on water and energy cycle. The impact of these activities on the SM have been well illustrated in a few studies (Jia et al., 2017; Liu et al., 2015; Qiu et al., 2016). One of the possible ways to reduce model uncertainties is by coupling other processes (e.g., dynamic vegetation and agricultural irrigation) in the VIC model which could potentially improve model performance for detecting hydrological systems and the disturbance from human activities (Luo et al., 2013; Xie et al., 2015).

The hydrological sensitivity-based approach adopted in our work is a simple way that can approximate estimates of future SM changes. This approach is advantageous because it is applicable at various scales and, unlike the VIC model, it does not need model parameter calibration (Vano et al., 2012; Vano and Lettenmaier, 2013). Moreover, this method is less time consuming than the full-simulation methods of conventional hydrological models. However, this approach may have substantial uncertainties in determining the effect of climate on the SM which may arise from various sources such as emission scenarios (Maurer, 2007). The selection of various climate scenarios is also one of the uncertainties for off-line modeling. Some other climate factors, such as short and long wave radiation, humidity, and wind field, may also impose effects on SM dynamics. Therefore, more factors related to the SM dynamics should be included in the approach. Moreover, the performance of this approach depends on the effectiveness of land surface models (the VIC simulation in this study) and the future climate scenarios. The land surface models may achieve different simulations due to different physics process and structures. Therefore, uncertainty exists in future SM estimation. It is necessary to compare those outputs in the following studies to deepen the understanding about SM sensitivity in response to P and T.

Piao et al. (2009b) indicated the amount of P in summer and the frequency were important factors of climate change that can induce SM changes. For example, the changes of P frequency could significantly affect hydrological and carbon cycles. However, only the amount of P was considered in this study which may not explain the SM dynamics completely. This also raised the uncertainty of results to analyze SM changes and sensitivity. Therefore, the amount and frequency of P, T and other related factors (e.g., humid, irrigation) should be considered in the sensitivity-based approach. Nevertheless, we provided a reliable range, instead of a single value, for projection of the SM dynamics as a response to climate change. Additionally, the results are consistent with the estimates from other studies that were based on complex land surface process models (Nakaegawa, 2017; Tao et al., 2003).

5. Conclusions

During the past decades, the SM in China has exhibited obvious spatio-temporal changes in response to climate change. In this study, the VIC model was applied to simulate the SM in China and its sensitivities to two critical climate factors, i.e., P and T, were quantified. Moreover, a sensitivity-based approach that is simple but effective to project future patterns of SM changes at the regional scale was presented. The conclusions from this study are as follows:

1. The VIC simulated SM was successfully evaluated using in-situ SM observations and satellite RS product (ESA-CCI SM). The results indicate that the simulations were capable of capturing the SM state in different layers and its seasonal variations. Therefore, the VIC simulations are suitable for projecting SM changes and conducting sensitivity analyses.
2. The temporal trend of SM showed obvious spatial heterogeneity as a response to P and T during the past five decades. Despite the rising T in China, SM continued increase at an average rate about 0.0065 mm/yr because of the increasing P (0.22 mm/yr). In particular, the SM in North West China increased to 0.047 mm/yr corresponding to the increasing P (0.94 mm/yr). In contrast, the SM in South West China has significantly decreased at a rate of −0.20 mm/yr. Therefore, the SM variation was primarily dominated by P as indicated by their strong correlation in each region.
3. The ε and *S* for each region were formulated to quantify the strength of the SM response to climate change in China and were calculated to be 0.25 (1% ΔP) and −3.21 (0.1 °C ΔT), respectively. The highest values were indicated in South East China (characterized by humid climate), indicating that the SM was most sensitive to P and T in the humid region.
4. The simple sensitivity-based approach could provide SM estimates consistent with the VIC simulations. Therefore, it is capable of projecting the SM values. Considering the expected changes in P and rise in the T from 2020 to 2050, SM is likely to decline significantly in South West China ($-5.95\% \pm 2.04\%$), while a slight increase may occur in the humid regions, i.e., South East China.

Uncertainties may exist in this study with respect to the SM response to climate change and the sensitivity-based projection. The VIC simulation did not consider the land use and land cover changes contributed by the climate system and anthropogenic activities (Xie et al., 2015). This study only quantified the impact of P amount rather the frequency, which may lead to significant consequences for SM dynamics (Piao et al., 2009a; Wu et al., 2012).

Moreover, the sensitivity-based approach only presented a regional scale projection and its performance depended on the hydrological model and climate scenarios. Our future work is expected to couple vegetation dynamics and anthropogenic activity impacts (e.g., urbanization and agricultural irrigation). The sensitivity-based approach should be evaluated with a full-simulation approach which is driven by output from GCMs.

Declaration of competing interests

The authors declare that they have no known competing financial interests or personal relationships that could have appeared to influence the work reported in this paper.

Acknowledgements

This study was supported by grants from the National Key Research and Development Program of China (No. 2016YFC0401404) and the National Natural Science Foundation of China (No. 41971030).

Appendix A. Supplementary data

Supplementary data to this article can be found online at https://doi.org/10.1016/j.scitotenv.2019.135774.

References

Alamusa, Y.T., Cao, J., Wang, Y., Liu, Y., 2017. Soil moisture influences vegetation distribution patterns in sand dunes of the Horqin Sandy Land, Northeast China. Ecol. Eng. 105, 95–101.

Amin, M.Z.M., Shaaban, A.J., Ercan, A., Ishida, K., Kavvas, M.L., Chen, Z.Q., et al., 2017. Future climate change impact assessment of watershed scale hydrologic processes in Peninsular Malaysia by a regional climate model coupled with a physically-based hydrology modelo. Sci. Total Environ. 575, 12–22.

Blum, W.E.H., 2013. Soil and land resources for agricultural production: general trends and future scenarios-a worldwide perspective. International Soil and Water Conservation Research 1, 1–14.

Cao, D., Shi, B., Zhu, H., Wei, G., Chen, S.-E., Yan, J., 2015. A distributed measurement method for in-situ soil moisture content by using carbon-fiber heated cable. J. Rock Mech. Geotech. Eng. 7, 700–707.

Chen, C., Lei, C., Deng, A., Qian, C., Hoogmoed, W., Zhang, W., 2011. Will higher minimum temperatures increase corn production in Northeast China? An analysis of historical data over 1965–2008. Agric. For. Meteorol. 151, 1580–1588.

Chiristensen, N.S., Lettenmaier, D.P., 2007. A multimodel ensemble approach to assessment of climate change impacts on the hydrology and water resources of the Colorado River basin. Hydrol. Earth Syst. Sci. 11, 17.

Dorigo, W.A., Gruber, A., De Jeu, R.A.M., Wagner, W., Stacke, T., Loew, A., et al., 2015. Evaluation of the ESA CCI soil moisture product using ground-based observations. Remote Sens. Environ. 162, 380–395.

FAO RILaWDD, 1998. Digital Soil Map of the World and Derived Soil Properties.

Haddeland, I., Skaugen, T., Lettenmaier, D.P., 2007. Hydrologic effects of land and water management in North America and Asia: 1700–1992. Hydrol. Earth Syst. Sci. Discuss. 3, 2899–2922.

Hansen, M.C., Defries, R.S., Townshend, J.R.G., Sohlberg, R., 2010. Global land cover classification at 1 km spatial resolution using a classification tree approach. Int. J. Remote Sens. 21, 1331–1364.

Jia, X., Ma, S., Zhu, Y., Luo, Y., 2017. Soil moisture decline due to afforestation across the Loess Plateau, China. J. Hydrol. 546, 113–122.

Jia, B., Liu, J., Xie, Z., Shi, C., 2018. Interannual variations and trends in remotely sensed and modeled soil moisture in China. J. Hydrometeorol. 19, 831–847.

Jiang, Y., 2015. China's water security: current status, emerging challenges and future prospects. Environ. Sci. Pol. 54, 106–125.

Jones, R.N., Chiew, F.H.S., Boughton, W.C., Zhang, L., 2006. Estimating the sensitivity of mean annual runoff to climate change using selected hydrological models. Adv. Water Resour. 29, 1419–1429.

Karthikeyan, L., Pan, M., Wanders, N., Kumar, D.N., Wood, E.F., 2017a. Four decades of microwave satellite soil moisture observations: part 1. A review of retrieval algorithms. Adv. Water Resour. 109, 106–120.

Karthikeyan, L., Pan, M., Wanders, N., Kumar, D.N., Wood, E.F., 2017b. Four decades of microwave satellite soil moisture observations: part 2. Product validation and intersatellite comparisons. Adv. Water Resour. 109, 236–252.

Koch, J., Cornelissen, T., Fang, Z., Bogena, H., Diekkrüger, B., Kollet, S., et al., 2016. Intercomparison of three distributed hydrological models with respect to seasonal variability of soil moisture patterns at a small forested catchment. J. Hydrol. 533, 234–249.

Leng, G., Tang, Q., Rayburg, S., 2015. Climate change impacts on meteorological, agricultural and hydrological droughts in China. Glob. Planet. Chang. 126, 23–34.

Li, B., Chen, Y., Chen, Z., Xiong, H., Lian, L., 2016a. Why does precipitation in northwest China show a significant increasing trend from 1960 to 2010? Atmos. Res. 167, 275–284.

Li, S., Liang, W., Zhang, W., Liu, Q., 2016b. Response of soil moisture to hydrometeorological variables under different precipitation gradients in the Yellow River Basin. Water Resour. Manag. 30, 1867–1884.

Liang, X., Xie, Z., 2001. A new surface runoff parameterization with subgrib-scale soil heterogeneity for land surface models. Adv. Water Resour. 24, 1173–1193.

Liang, X., Xie, Z., 2003. Important factors in land–atmosphere interactions: surface runoff generations and interactions between surface and groundwater. Glob. Planet. Chang. 38, 101–114.

Liang, X., Lettenmaier, D.P., Wood, E.F., Burges, S.J., 1994. A simple hydrologically based model of land surface water and energy fluxes for general circulation models. J. Geophys. Res. 99 (D7), 14.

Liang, X., Wood, E.F., Lettenmaier, D.P., 1996. Surface soil moisture parameterization of the VIC-2L model: evaluation and modification. Glob. Planet. Chang. 13 (1–4), 195–206.

Liu, Y., Pan, Z., Zhuang, Q., Miralles, D.G., Teuling, A.J., Zhang, T., et al., 2015. Agriculture intensifies soil moisture decline in Northern China. Sci. Rep. 5.

Liu, S.-L., Pu, C., Ren, Y.-X., Zhao, X.-L., Zhao, X., Chen, F., et al., 2016. Yield variation of double-rice in response to climate change in Southern China. Eur. J. Agron. 81, 161–168.

Luo, X., Liang, X., McCarthy, H.R., 2013. VIC+ for water-limited conditions: a study of biological and hydrological processes and their interactions in soil-plant-atmosphere continuum. Water Resour. Res. 49, 7711–7732.

Maurer, E.P., 2007. Uncertainty in hydrologic impacts of climate change in the Sierra Nevada, California, under two emissions scenarios. Clim. Chang. 82, 309–325.

Mishra, A., Vu, T., Veettil, A.V., Entekhabi, D., 2017. Drought monitoring with soil moisture active passive (SMAP) measurements. J. Hydrol. 552, 620–632.

Nakaegawa, T., 2017. Statistical evaluation of future soil moisture changes in East Asia projected in a CMIP5 multi-model ensemble. Hydrological Research Letters 11, 37–43.

Nijssen, B., Schnur, R., Lettenmaier, D.P., 2001. Global retrospective estimation of soil moisture using the variable infiltration capacity land surface model, 1980–93. J. Clim. 14, 1790–1808.

Piao, S., Lei, Y., Wang, X., Ciais, P., Peng, S., Shen, Z., et al., 2009a. Summer soil moisture regulated by precipitation frequency in China. Environ. Res. Lett. 4, 549–567.

Piao, S., Yin, L., Wang, X., Ciais, P., Peng, S., Shen, Z., et al., 2009b. Summer soil moisture regulated by precipitation frequency in China. Environ. Res. Lett. 4, 044012.

Piao, S., Ciais, P., Huang, Y., Shen, Z., Peng, S., Li, J., et al., 2010. The impacts of climate change on water resources and agriculture in China. Nature 467, 43–51.

Qiu, J., Gao, Q., Wang, S., Su, Z., 2016. Comparison of temporal trends from multiple soil moisture data sets and precipitation: the implication of irrigation on regional soil moisture trend. Int. J. Appl. Earth Obs. Geoinf. 48, 17–27.

Rushton, K.R., Eilers, V.H.M., Carter, R.C., 2006. Improved soil moisture balance methodology for recharge estimation. J. Hydrol. 318, 379–399.

Seneviratne, S.I., Corti, T., Davin, E.L., Hirschi, M., Jaeger, E.B., Lehner, I., et al., 2010. Investigating soil moisture–climate interactions in a changing climate: a review. Earth Sci. Rev. 99, 125–161.

She, D., Liu, D., Xia, Y., Ma, S., 2014. Modeling effects of land use and vegetation density on soil water dynamics: implications on water resource management. Water Resour. Manag. 28, 2063–2076.

Stoll, S., Hendricks Franssen, H.-J., Bárdossy, A., Kinzelbach, W., 2013. On the relationship between atmospheric circulation patterns, recharge and soil moisture dynamics in Switzerland. J. Hydrol. 502, 1–9.

Tang, C., Dennis, R.L., 2014. How reliable is the offline linkage of Weather Research & Forecasting Model (WRF) and variable infiltration capacity (VIC) model? Glob. Planet. Chang. 116, 1–9.

Tang, C., Piechota, T.C., 2009. Spatial and temporal soil moisture and drought variability in the Upper Colorado River Basin. J. Hydrol. 379, 122–135.

Tao, F., Yokozawa, M., Hayashi, Y., Lin, E., 2003. Future climate change, the agricultural water cycle, and agricultural production in China. Agric. Ecosyst. Environ. 95, 203–215.

Thompson, S.E., Harman, C.J., Heine, P., Katul, G.G., 2010. Vegetation-infiltration relationships across climatic and soil type gradients. Journal of Geophysical Research: Biogeosciences 115 (n/a-n/a).

Tian, Q., Yang, S., 2017. Regional climatic response to global warming: trends in temperature and precipitation in the Yellow, Yangtze and Pearl River basins since the 1950s. Quat. Int. 440, 1–11.

Tian, Q., Prange, M., Merkel, U., 2016. Precipitation and temperature changes in the major Chinese river basins during 1957–2013 and links to sea surface temperature. J. Hydrol. 536, 208–221.

Touhami, I., Chirino, E., Andreu, J.M., Sánchez, J.R., Moutahir, H., Bellot, J., 2015. Assessment of climate change impacts on soil water balance and aquifer recharge in a semi-arid region in south east Spain. J. Hydrol. 527, 619–629.

Vano, J.A., Lettenmaier, D.P., 2013. A sensitivity-based approach to evaluating future changes in Colorado River discharge. Clim. Chang. 122, 621–634.

Vano, J.A., Das, T., Lettenmaier, D.P., 2012. Hydrologic sensitivities of Colorado River runoff to changes in precipitation and temperature. J. Hydrometeorol. 13, 932–949.

Vano, J.A., Nijssen, B., Lettenmaier, D.P., 2015. Seasonal hydrologic responses to climate change in the Pacific Northwest. Water Resour. Res. 51, 1959–1976.

Wang, A., Lettenmaier, D.P., Sheffield, J., 2011. Soil moisture drought in China, 1950–2006. J. Clim. 24, 3257–3271.

Wang, G.Q., Zhang, J.Y., Jin, J.L., Pagano, T.C., Calow, R., Bao, Z.X., et al., 2012. Assessing water resources in China using PRECIS projections and a VIC model. Hydrol. Earth Syst. Sci. 16, 231–240.

Wang, L., Chen, W., Zhou, W., 2014. Assessment of future drought in Southwest China based on CMIP5 multimodel projections. Adv. Atmos. Sci. 31, 1035–1050.

Wang, S., Mo, X., Liu, S., Lin, Z., Hu, S., 2016. Validation and trend analysis of ECV soil moisture data on cropland in North China Plain during 1981–2010. Int. J. Appl. Earth Obs. Geoinf. 48, 110–121.

Wu, C., Chen, J.M., Pumpanen, J., Cescatti, A., Marcolla, B., Blanken, P.D., et al., 2012. An underestimated role of precipitation frequency in regulating summer soil moisture. Environ. Res. Lett. 7, 024011.

Wu, H., Adler, R.F., Tian, Y., Huffman, G.J., Li, H., Wang, J., 2014. Real-time global flood estimation using satellite-based precipitation and a coupled land surface and routing model. Water Resour. Res. 50, 2693–2717.

Xie, Z., Yuan, F., Duan, Q., Zheng, J., Liang, M., Chen, F., 2007. Regional parameter estimation of the VIC land surface model: methodology and application to River Basins in China. J. Hydrometeorol. 8, 447–468.

Xie, X., Liang, S., Yao, Y., Jia, K., Meng, S., Li, J., 2015. Detection and attribution of changes in hydrological cycle over the Three-North region of China: climate change versus afforestation effect. Agric. For. Meteorol. 203, 74–87.

Yan, G., Wen-Jie, D., Fu-Min, R., Zong-Ci, Z., Jian-Bin, H., 2013. Surface air temperature simulations over China with CMIP5 and CMIP3. Adv. Clim. Chang. Res. 4, 145–152.

Zhai, P., Zhang, X., Wan, H., Pan, X., 2005. Trends in total precipitation and frequency of daily precipitation extremes over China. J. Clim. 18, 1096–1108.

Zhang, X., Tang, Q., Pan, M., Tang, Y., 2014. A long-term land surface hydrologic fluxes and states dataset for China. J. Hydrometeorol. 15, 2067–2084.

Zhang, H.-L., Zhao, X., Yin, X.-G., Liu, S.-L., Xue, J.-F., Wang, M., et al., 2015. Challenges and adaptations of farming to climate change in the North China Plain. Clim. Chang. 129, 213–224.

Zhang, S., Shao, M., Li, D., 2017. Prediction of soil moisture scarcity using sequential Gaussian simulation in an arid region of China. Geoderma 295, 119–128.

Zribi, M., 2003. Surface soil moisture estimation from the synergistic use of the (multi-incidence and multi-resolution) active microwave ERS wind Scatterometer and SAR data. Remote Sens. Environ. 86, 30–41.